Int J Mater Form (2009) Vol. 2 Suppl 1:539–542
DOI 10.1007/s12289-009-0490-0

MODELLING OF A BURR-FREE BLANKING PROCESS

H.H.Wisselink[1,3] *, **G.Klaseboer**[2], **H. Huétink**[3]

[1] Materials Innovation Institute (M2i),P.O. Box 5008, 2600GA Delft, The Netherlands
[2] Advanced Technology Center, Philips CL, Tussendiepen 4, 9206 AD Drachten, The Netherlands
[3] Faculty of Engineering Technology, University of Twente (UT),P.O. Box 217, 7500AE Enschede, The Netherlands

ABSTRACT: A two step burr-free blanking process is investigated, where the deformation due to the preceding deep-drawing process is taken into account. FEM simulations have been carried out using a nonlocal damage model to obtain mesh independent results. It is shown how the parameters of the damage model influence the failure in the blanking process. Furthermore the simulations are validated with the measured contour and hardness of the part in different stages of the process.

KEYWORDS: Burrfree blanking, nonlocal damage

1 INTRODUCTION

The last step in a multi step metal forming process using progressive tooling as shown in Figure 1 is the separation of the finished parts from the strip of steel. To obtain a burr-free product this blanking process is carried out in two steps [1]. First a groove is pressed into the sheet and next the grooved sheet is blanked from the opposite direction. Now smooth edges are obtained with a fractured part located in the middle of the sheet, where in conventional blanking a burr is formed at one of the edges.
The objective is to avoid separation during groove forming and obtain separation during blanking. This process is modelled to investigate the consequences of the selection of other materials, with different ductility than the currently used ones, on the sheared edge of the product and the robustness of the process.

2 FEM MODEL

During the last ten years a lot of articles have appeared on the FEM simulation of blanking, which show a variety of damage models, remeshing and crack propagation algorithms. Some recent articles are [2–5].
The studied blanking process can be approximated with an axi-symmetric model. The following approach has been used:

1. The relevant forming steps before blanking (draw1 and draw2) are modelled with Crystal, an in house FEM code suitable for modelling multiple forming steps, to obtain a good estimate of the state variables before groove forming.

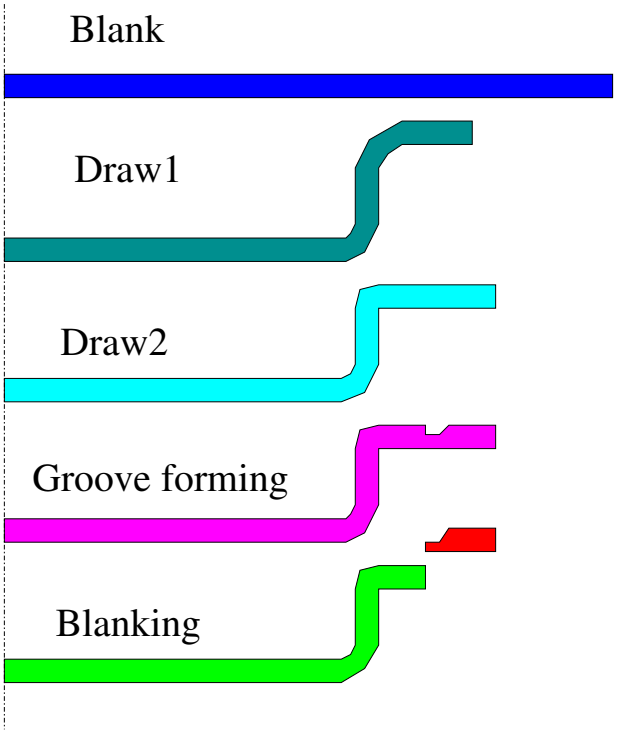

Figure 1: *The investigated multi-step forming process.*

2. The burr-free blanking (groove forming and blanking) is modelled with the explicit FEM code LS-DYNA. A limited domain, a ring of material around the blanking zone, is used with an initial state based on the previous forming steps.

Here a nonlocal damage model is applied, which will be described in Section 3. Remeshing is used and crack prop-

*Corresponding author: P.O. Box 217, 7500AE Enschede, The Netherlands, +31 (0)53-4892545, h.wisselink@m2i.nl

agation is modelled with an element kill procedure for completely damaged elements.

3 NONLOCAL DAMAGE MODEL

The nonlocal damage model presented here is based on the work of Mediavilla et al. [6]. Nonlocal damage models are used to avoid the mesh dependency problems of local damage models. The local damage driving variable z is a function of the local stress and strain history as defined in Equation 1. The triaxiality $\frac{\sigma_h}{\sigma_{eq}}$ in this equation proves to be important factor [7].

$$z = \int_{\varepsilon_p} \langle 1 + A\frac{\sigma_h}{\sigma_{eq}} \rangle \varepsilon_p^B d\varepsilon_p \tag{1}$$

The nonlocal damage driving variable $\bar{z}$ is obtained using a Helmholtz partial differential equation with a Neumann boundary condition (Equation 2). l is the internal length scale, which controls the width of the localisation bands and $\mathbf{n}$ the outward normal on the boundary Γ.

$$\bar{z} - l^2\nabla^2\bar{z} = z; \quad \nabla\bar{z}\cdot\mathbf{n} = \mathbf{0} \quad \text{on } \boldsymbol{\Gamma} \tag{2}$$

The evolution of history parameter κ is according the Kuhn-Tucker loading-unloading conditions.

$$\dot{\kappa} \geq 0; \quad \bar{z} - \kappa \leq 0; \quad \dot{\kappa}(\bar{z} - \kappa) = 0 \tag{3}$$

The degradation of the material properties ω is calculated from the history parameter κ using a damage evolution law. Here a linear law is used, the degradation initiates at κ_i and the material fails completely at κ_u.

$$\begin{aligned} \omega &= 0 \quad \text{for} \quad \kappa < \kappa_i \\ \omega &= \frac{\kappa - \kappa_i}{\kappa_u - \kappa_i} \quad \kappa_i \leq \kappa \leq \kappa_u \\ \omega &= 1 \quad \text{for} \quad \kappa > \kappa_u \end{aligned} \tag{4}$$

The yield stress is calculated using a strain hardening function h, which competes with the softening due to damage.

$$\sigma_y = (1 - \omega)h(\varepsilon_p) \tag{5}$$

This damage model is implemented in LS-DYNA, using the user subroutines UMAT43 and UCTRL1. An operator split method is applied in which the damage is kept constant during an increment. The calculation of the nonlocal damage from Equation 2, which requires the solution of a system of equations, takes relatively much time compared to the time needed for one increment in an explicit FEM code. Therefore the nonlocal damage is only updated every n-th (typical 100) increment.
The material used in this paper is a martensitic stainless steel in the annealed (ferritic) state. The initial hardness is 140 HV. An isotropic VonMises model is used with Nadai hardening (Equation 6). Strain-rate effects are not taken into account.

$$\begin{aligned} h(\varepsilon_p) &= 818(-8.5\cdot10^{-3} + \varepsilon_p)^{0.217} \\ h(\varepsilon_p) &= \min(270, h(\varepsilon_p)) \end{aligned} \tag{6}$$

The parameters of the damage model (Table 1) are not determined experimentally yet. The length scale l is a material parameter, which determines the width of localisation bands. The larger the value of l the more ductile is the response of the material. However the nonlocal model requires that the used element size in the simulation has to be smaller than l. Therefore often some compromise is made between accuracy and efficiency, but a too large length scale leads to non-physical behaviour. Different values of κ_i and κ_u have been used.

Table 1: *Damage parameters*

A	3.0	l	10 μm
B	0.0	κ_i	1.0-2.0
		κ_u	4.0-8.0

4 RESULTS

Tests have been carried out in the production line. The punch displacement has been adapted to create samples in different stages of groove forming and blanking. The final depth of the groove is about half the sheet thickness. The clearance for blanking is 14% of the initial sheet thickness. From all samples the contour of a cross-section and the hardness has been measured. These data will be used to validate the simulation results.
The size of the initial ring shape before groove forming simulation is based on the deepdrawing simulations and agrees with the measured shape as shown in Figure 2. The outer diameter decreases and the thickness increases about 10% during the drawing steps.

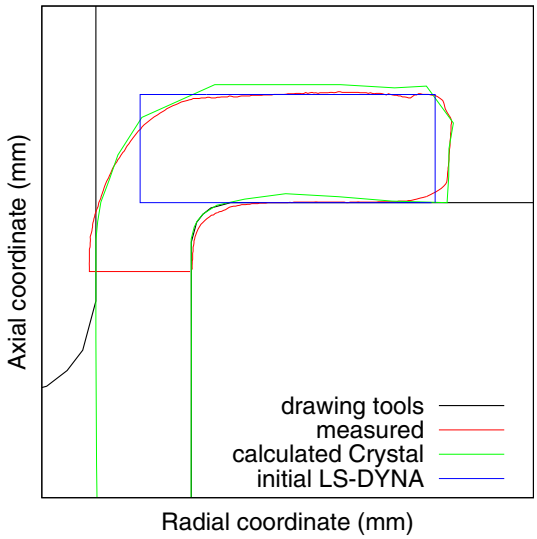

Figure 2: *Shape before groove forming.*

A constant initial plastic strain $\varepsilon_p = 0.3$ is used in the groove forming simulations, which is an average of the plastic strain in the flange at the end of the drawing steps.

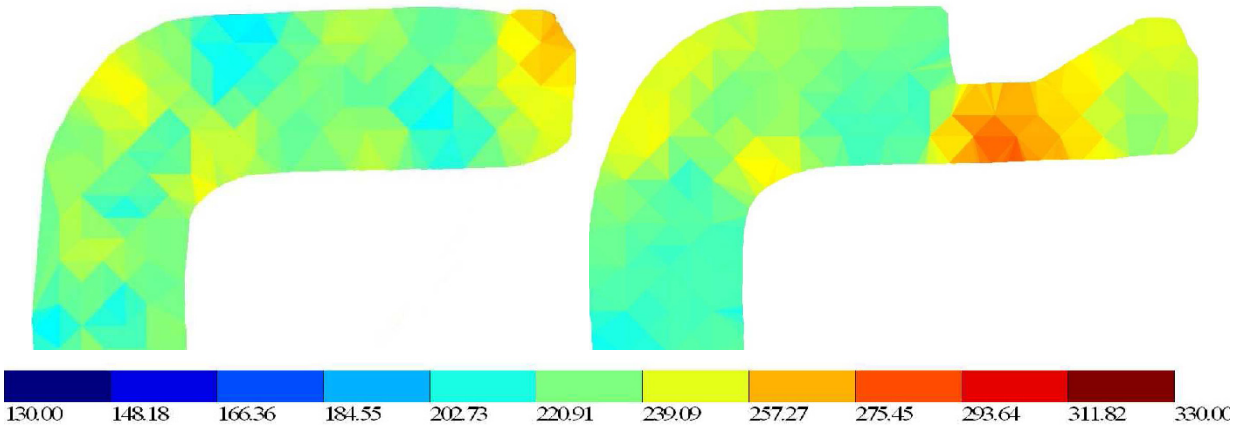

Figure 3: *Measured hardness (HV) before and after groove forming.*

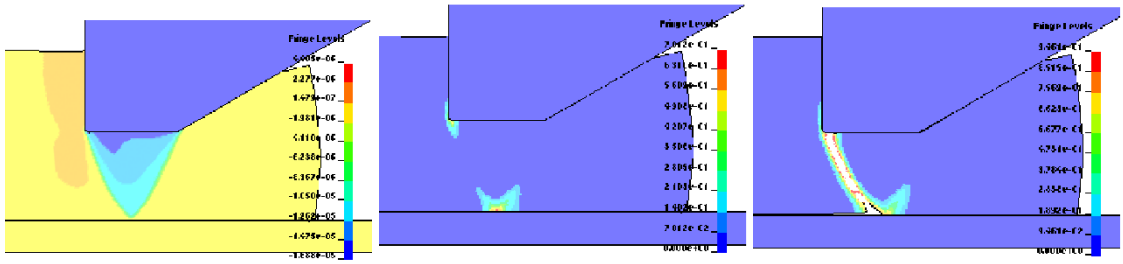

Figure 4: *Axial-displacement (left) and degradation ω in groove forming before (middle) and after failure (right), $\kappa_i = 1; \kappa_u = 4$.*

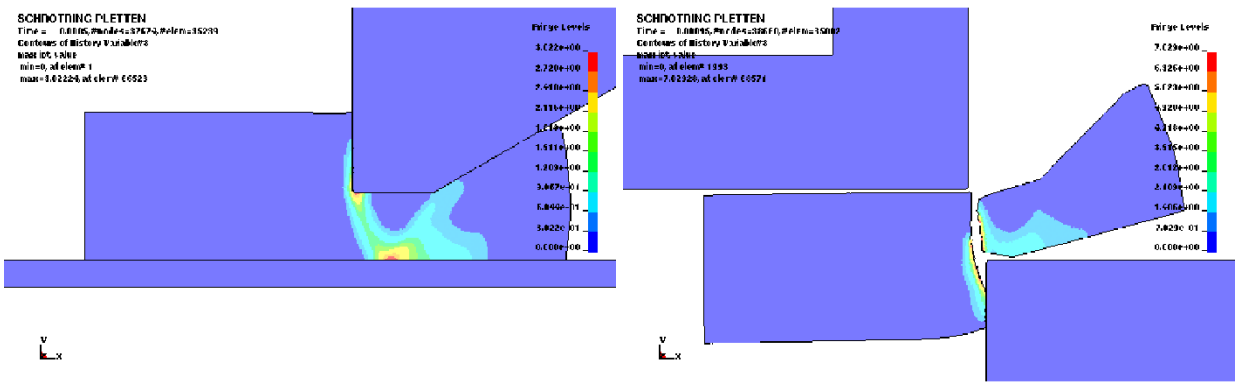

Figure 5: *Nonlocal damage $\bar{z}$ after groove forming (left) and blanking (right), $\kappa_i = 2; \kappa_u = 8$.*

It is assumed that no damage has been developed during drawing as the triaxiality in the flange is negative. The deformation due to conventional blanking of the outer edge before drawing is not taken into account, but is clearly visible in the measurements. The radial displacement of the boundary at the inner radius is suppressed at sufficient distance from the deformation zone. Remeshing is used with a constant mesh size of $5\mu m$, which leads to a total number of about 35000 elements. A Coulomb friction coefficient of 0.1 is applied for the contact with the rigid tools.

During groove forming the deformation will localise into a shear band as shown in Figure 4. The groove depth at which failure occurs depends on the the ductility of the material, punch shape and the prestrain from the previous drawing process [8]. This prestrain reduces the obtainable groove depth.

The hardness before and after groove forming, given in

Figure 3, shows an increase in hardness in the groove, but the resolution is not large enough to capture any shear bands. The material is mainly pushed outwards (Figure 6), which supports the assumption that the blanking process can be modeled on a limited domain.

Increasing the ductility by selecting larger, more realistic values for κ_i and κ_u postpones the failure. Now failure is avoided during groove forming and the separation occurs during the blanking operation (Figure 5). The measured and calculated contours after blanking have a similar shape as shown in Figure 7. The used outer radius of the ring before groove forming has been taken too small, which difference can be seen in all stages of the process.

Phenomena like tool wear, tool deformation and misalignment, which seem to be present in the measured contours, leads to small deviations between simulations and experiments.

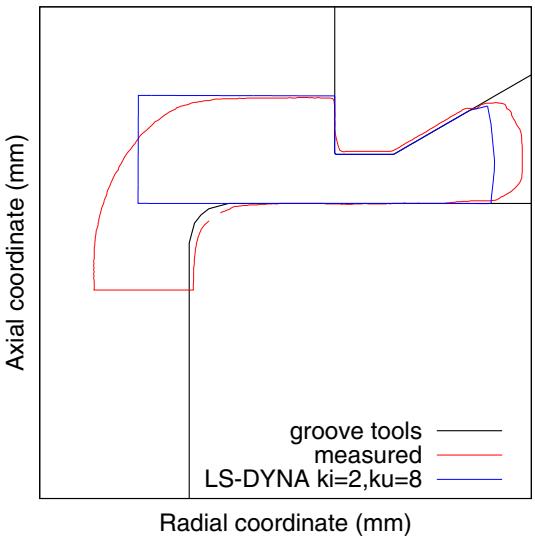

Figure 6: *Shape after groove forming.*

5 CONCLUSIONS

The burr-free blanking process can be simulated completely using the described FEM model. The nonlocal damage model gives a meshsize independent solution. The results agree with the measured data, but can be improved with more accurate material and process data. The damage parameters should be determined experimentally to increase the predictive capabilities of the model.

ACKNOWLEDGEMENT

This research was carried out under the project number MC1.05205 in the framework of the Research Program of the Materials innovation institute M2i (www.m2i.nl), the former Netherlands Institute for Metals Research.

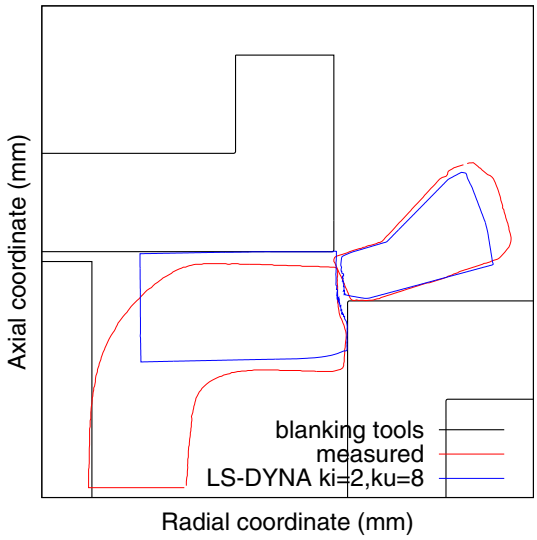

Figure 7: *Shape after blanking.*

REFERENCES

[1] K. Kondo. Recent developments of shearing in Japan. *Int. J. Mach. Tools Manufact.*, 29:29–38, 1989.

[2] Song Yu, Xiaolong Xie, Jie Zhang, and Zhen Zhao. Ductile fracture modeling of initiation and propagation in sheet-metal blanking processes. *J. Mat. Proc. Tech.*, 187-188:169–172, 2007.

[3] V. Lemiale, J. Chamberta, and P. Picart. Description of numerical techniques with the aim of predicting the sheet metal blanking process by FEM simulation. *J. Mat. Proc. Tech.*, ?:?–?, 2008.

[4] H. Marouani, A. Ben Ismail, E. Hugc, and M. Rachik. Rate-dependent constitutive model for sheet metal blanking investigation. *Materials Science and Engineering A*, 487:162–170, 2008.

[5] A. Dalloz, J. Besson, A.-F. Gourgues-Lorenzon, T. Sturel, and A. Pineau. Effect of shear cutting on ductility of a dual phase steel. *Engineering Fracture Mechanics*, ?:?–?, 2009.

[6] J. Mediavilla, R.H.J. Peerlings, and M.G.D. Geers. An integrated continuous-discontinuous approach towards damage engineering in sheet metal forming processes. *Engineering Fracture Mechanics*, 73(7): 895–916, May 2006.

[7] A.M. Goijaerts, L.E. Govaert, and F.P.T. Baaijens. Characterisation of ductile fracture in metal blanking. *J. Mat. Proc. Tech.*, 110:312–323, 2001.

[8] S.H.A. Boers, P.J.G. Schreurs, and M.G.D. Geers. Operator-split damage-plasticity applied to groove forming in food can lids. *Int. J. of Solids and Structures*, 42:4154–4178, 2005.